Inorg. Chem. **2005**, *44*, 2443–2453

Synthesis, Structural Characterization, and Photophysical Properties of Palladium and Platinum(II) Complexes Containing 7,8-Benzoquinolinate and Various Phosphine Ligands

Alvaro Díez,[†] Juan Forniés,*[,‡] Ana García,[†] Elena Lalinde,*[,†] and M. Teresa Moreno[†]

Departamento de Química-Grupo de Síntesis Química de La Rioja, UA-CSIC, Universidad de La Rioja, 26006, Logroño, Spain, and Departamento de Química Inorgánica, Instituto de Ciencia de Materiales de Aragón, Universidad de Zaragoza-Consejo Superior de Investigaciones Científicas, 50009 Zaragoza, Spain

Received December 9, 2004

A series of mononuclear cyclometalated benzo[*h*]quinolinate platinum and palladium(II) complexes with phosphine ligands, namely, [M(bzq)ClL] (L = PPh_2H, Pt **1**, Pd **2**; $PPh_2C{\equiv}CPh$, Pt **3**, Pd **4**), $[Pt(bzq)(PPh_2H)(PPh_2C{\equiv}CPh)]ClO_4$ **5**, $[Pt(bzq)(PPh_2C(Ph){=}C(H)PPh_2)]ClO_4$ **6**, and $[Pt(bzq)(C{\equiv}CPh)(PPh_2C{\equiv}CPh)]$ (**7a**, **7b**), were synthesized. The X-ray crystal structures of **1**, **6**·CH_3COCH_3·$^1/_2CH_3(CH_2)_4CH_3$, and **7b**·CH_3COCH_3 have been determined. In **1**, the metalated carbon atom and the P atom are mutually cis, whereas in **7b** they are trans located. For complex **6**, C and N are crystallographically indistinguishable. Reaction of $[Pt(bzq)(\mu\text{-}Cl)]_2$ with PPh_2H and excess of NEt_3 leads to the phosphide-bridge platinum dimer $[Pt(bzq)(\mu\text{-}PPh_2)]_2$ **8** (X-ray). Moderate π–π intermolecular interactions and no evident Pt–Pt interactions are found in **1**, **7b**, and in **8**. All of the complexes exhibit absorption bands at high energy due to the intraligand transitions (^{1}IL $\pi \rightarrow \pi^*$) and absorptions at lower energy which are attributed to MLCT (5d) $\pi \rightarrow \pi^*$ (C^N) transition. Platinum complexes show strong luminescence in both solid state and frozen solutions. The influence of the coligands on the photophysics of the platinum complexes has been examined by absorption and emission spectroscopy.

Introduction

The chemistry of Pt(II) and Pd(II) complexes containing cyclometalated ligands has attracted great interest in recent years due to their applications in different areas.[1−9] In particular, a significant research effort has focused on the study of platinum complexes mainly due to the potential antitumor activity[9−12] of some of these complexes and their interesting photophysical properties. Compared with the palladium analogue, the Pt(II) complexes benefit from having higher energy, metal-centered (MC) or ligand-field excited states that do not serve in deactivation pathways from intraligand and MLCT emissive states. The strong spin−orbit coupling of the heavy Pt atom allows for efficient mixing of the ^{1}MLCT with the ^{3}MLCT and $^3\pi\pi$ excited states thus leading to high efficiency and long luminescent lifetimes of the emissive states that are very attractive in materials science.[13−36]

* Corresponding authors. E-mail: elena.lalinde@dq.unirioja.es (E.L.); forniesj@posta.unizar.es (J.F.).
† Universidad de La Rioja, UA-CSIC.
‡ Universidad de Zaragoza-CSIC.

(1) Espinet, P.; Esteruelas, M. A.; Oro, L. A.; Serrano, J. L.; Sola, E. *Coord. Chem. Rev.* **1992**, *117*, 215.
(2) Omae, I. *Coord. Chem. Rev.* **1988**, *83*, 137.
(3) Omae, I. *Applications of Organometallic Compounds*; Wiley: Chichester, U.K., 1998.
(4) Ryabov, A. D. *Chem. Rev.* **1990**, *90*, 403.
(5) Newkome, G. R.; Puckett, W. E.; Gupta, V. K.; Kiefer, G. E. *Chem. Rev.* **1986**, *86*, 451.
(6) Wild, S. B. *Coord. Chem. Rev.* **1997**, *166*, 291.
(7) Spencer, J.; Pfeffer, M. *Adv. Organomet. Chem.* **1998**, *6*, 103.
(8) Dupont, J.; Pfeffer, M.; Spencer, J. *Eur. J. Inorg. Chem.* **2001**, 1917.
(9) Hambley, T. *Coord. Chem. Rev.* **1997**, *166*, 118.
(10) Ranatunge-Bandarage, P. R. R.; Duffy, N. N.; Johnson, S. J.; Simpson, J. *Organometallics* **1994**, *13*, 511.
(11) Navarro-Ranninger, C.; López Solera, I.; González, V. M.; Pérez, J. M.; Alvarez-Valdes, A.; Martín, A.; Raithby, P. R.; Masaguer, J. R.; Alonso, C. *Inorg. Chem.* **1996**, *35*, 5181.
(12) Headford, C. E.; Mason, R.; Ranatunge-Bandarage, P. R. R.; Robinson, B. H.; Simpson, J. *J. Chem. Soc., Chem. Commun.* **1990**, 601.
(13) Chan, C. W.; Cheng, L. K.; Che, C. M. *Coord. Chem. Rev.* **1994**, *132*, 87.
(14) Craig, C. A.; Garces, F. O.; Watts, R. J.; Palmans, R.; Frank, A. J. *Coord. Chem. Rev.* **1990**, *97*, 193.
(15) Brooks, J.; Babayan, Y.; Lamansky, S.; Djuorovich, P. I.; Tsyba, I.; Bau, R.; Thompson, M. E. *Inorg. Chem.* **2002**, *41*, 3055.
(16) Fernández, S.; Forniés, J.; Gil, B.; Gómez, J.; Lalinde, E. *J. Chem. Soc., Dalton Trans.* **2003**, 822.

10.1021/ic048272g CCC: $30.25 © 2005 American Chemical Society
Published on Web 02/24/2005

In addition, the open square-planar geometry of these d^8 molecules allows axial nucleophilic attack or intermolecular Pt···Pt stacking, facilitating other deactivating pathways in these complexes.[13,19,20,22,23,27] Furthermore, the influence of the noncovalent $\pi-\pi$ ligand contacts on the photoluminescence of these species has many precedents.[20−24] It has been shown that the nature of the ancillary ligands can have a strong effect on the lowest emitting excited state. In fact, the lowest energy excited state in these types of complexes has been attributed to ligand-centered ^{3}LC metal-to-ligand charge-transfer ^{3}MLCT, excimeric $^3(\pi\pi^*)$ metal−metal-to-ligand charge-transfer ^{3}MMLCT (or [d$\sigma^* \rightarrow \pi^*$]), and LL'CT.

Despite considerable advances in this area, few systems containing phosphine fragments have been studied.[29−32,37−39] Recently, we have described the synthesis and properties of heteroleptic bis(alkynyl)(benzoquinolinate)platinate(II) complexes,[16] whose emissions were proposed to arise from mixed [πC≡CR/Pt d/π(bzq) → π^*bzq] transitions on the basis of TD-DFT calculations. On heteroleptic phosphine C^N PtLX derivatives, the modification of charge, the electron-donating or -withdrawing character of the L or X ligand, and solubility can serve to tune the photophysical properties.

In this paper, we describe the synthesis and characterization of heteroleptic platinum and palladium(II) "M(C^N)" (C^N = 7,8-benzoquinolinate) complexes bearing the phosphine ligands, PPh_2H and/or $PPh_2C{\equiv}CPh$. In addition, the formation of the phosphido-bridged Pt(II) dimer [Pt(bzq)-(μ-PPh_2)]$_2$ is presented. Through ligand modification, the variations in photophysical properties (electronic absorption and luminescence) have been analyzed.

Experimental Section

General Procedures. All reactions were carried out under argon atmosphere, and solvents were dried by standard procedures and distilled before use. Proton, $^{13}C\{^1H\}$, and ^{31}P NMR spectra were recorded on a Bruker ARX-300 spectrometer with chemical shifts externally referenced to $SiMe_4$ and 85% H_3PO_4, working at 300.1 MHz for ^{1}H, at 121.5 MHz for ^{31}P, and at 100.6 MHz for $^{13}C\{^1H\}$. Infrared spectra were recorded with a Perkin-Elmer FT-IR 1000 spectrometer as Nujol mulls between polyethylene sheets, and C, H, and N analyses were carried out with a Carlo Erba EA1110 CHNS-O microanalyzer. Mass spectra were obtained on a HP-5989B mass spectrometer (ES technique), and conductivities were measured in acetone solutions (ca. 5×10^{-4} mol^{-1}) with a Crison GLP 31 conductimeter. UV−visible spectra were obtained on a Hewlet Packard 8453 spectrometer. Emission and excitation spectra were obtained on a Perkin-Elmer luminescence spectrometer LS 50B and on a Jobin-Yvon Horiba Fluorolog 3-11 Tau-3 spectrofluorimeter, in which the lifetime measurements were performed operating in the phosphorimeter mode. The precursors [Pt(bzq)(μ-Cl)]$_2$,[40] [Pd(bzq)(μ-Cl)]$_2$ [41] (bzqH = benzo[*h*]quinoline), and the ligand $PPh_2C{\equiv}CPh$[42] were prepared according to reported procedures. PPh_2H and HC≡CPh were used as received.

Synthesis of [Pt(bzq)Cl(PPh_2H)] (1). PPh_2H (84.7 μL, 0.489 mmol) was added to a yellow suspension of [Pt(bzq)(μ-Cl)]$_2$ (0.200 g, 0.245 mmol) in CH_2Cl_2 (20 mL) and stirred for 1 h. Evaporation of the solution to a small volume (2 mL) afforded a yellow solid. Yield: 0.220 g (76%). This was identified by NMR spectroscopy as **1** with small traces of the other isomer [^{1}H NMR δ 9.23, 8.72 (H^2, H^9, bzq)]. Crystallization from $CHCl_3$/hexane at −20 °C gave pure **1** as a microcrystalline yellow solid. Yield: 0.16 g (55%). Anal. Calcd for $C_{25}ClH_{19}NPPt$: C, 50.47; H, 3.22; N, 2.35. Found: C, 49.94; H, 3.06; N, 2.35. MS ES(+): *m*/*z* 560 [M − Cl]$^+$ 100%. IR (cm^{-1}): ν(P−H) 2364 (m); ν(Pt−Cl) 292 (m). ^{1}H NMR (δ, $CDCl_3$): 9.87 (m, $^3J_{Pt-H}$ = 26 Hz, H^2, bzq), 8.35 (d, J_{H-H} = 7.8 Hz, H^9, bzq), 7.93 (m, 4H, Ph/bzq), 7.77 (d, J_{H-H} = 8.7 Hz, bzq), 7.63 (m, 4H, Ph/bzq), 7.44 (m, 6H, Ph/bzq), 7.31 (m, 1H, Ph/bzq), 6.81 (d, $^1J_{P-H}$ = 414 Hz, $^2J_{Pt-H}$ = 41.3 Hz, 1H, PPh_2H; only one of the signals is seen, the other is overlapped with the aromatic signals. $^{31}P\{^1H\}$ NMR (δ, $CDCl_3$): −1.51 (s, $^1J_{Pt-P}$ = 4149 Hz). ^{31}P NMR (δ, $CDCl_3$): −1.28 (d, $^1J_{P-H}$ = 414 Hz, $^1J_{Pt-P}$ = 4150 Hz). $^{13}C\{^1H\}$ NMR (δ, $CDCl_3$): 154.8 (s, C^{10} bzq), 147.8 (s, $^2J_{Pt-C}$ = 28.3 Hz, C^2 bzq), 141.9 (s, $^2J_{Pt-C}$ = 22.0 Hz, C$^{13/14}$ bzq), 138.5 (s, C$^{3/4}$ (*C*H) bzq), 138.4 (s, C$^{13/14}$ bzq), 134.5 (d, $^2J_{C-P}$ = 11.2 Hz, $^3J_{Pt-C}$ = 31.6 Hz, C_{ortho} PPh_2), 134.2 (s, J_{Pt-C} = 35 Hz, C$^{11/12}$), 131.5 (d, $^3J_{C-P}$ = 9.6 Hz, $^2J_{Pt-C}$ = 94.9 Hz, C^9 bzq), 131.3 (d, $^4J_{C-P}$ = 2.5 Hz, C_{para} PPh_2), 129.7 (d, $^4J_{C-P}$ = 3.1 Hz, C^7 bzq), 129.4 (s, *C*H bzq), 128.8 (d, $^3J_{C-P}$ = 12.5 Hz, C_{meta} PPh_2), 126.7 (d, J_{C-P} = 2.0 Hz, $^2J_{Pt-C}$ = 26.4 Hz, C$^{11/12}$ bzq), 126.3 (d, $^1J_{P-C}$ = 62.3 Hz, $^2J_{Pt-C}$ = 27.2 Hz, C_{ipso}, PPh_2), 123.4 (s, *C*H bzq), 122.6 (s, *C*H bzq), 121.2 (d, $^4J_{C-P}$ = 3.8 Hz, $^3J_{C-Pt}$ = 25.8 Hz, C^8 bzq).

(17) Jolliet, P.; Gionini, M.; von Zelewsky, A.; Bernardinelly, G.; Stoeckli-Evans, H. *Inorg. Chem.* **1996**, *35*, 4883.
(18) Zheng, G. Y.; Rillema, D. P.; DePriest, J.; Woods, C. *Inorg. Chem.* **1998**, *37*, 3588.
(19) Lai, S. W.; Lam, H. W.; Lu, W.; Cheung, K. K.; Che, C. M. *Organometallics* **2002**, *21*, 226.
(20) Lu, W.; Chan, C. W.; Zhu, N.; Che, C. M.; Li, C.; Hui, Z. *J. Am. Chem. Soc.* **2004**, *126*, 7639.
(21) Lu, W.; Chan, M. C. W.; Cheung, K. K.; Che, C. M. *Organometallics* **2001**, *20*, 2477.
(22) Lu, W.; Mi, B. X.; Chan, M. C. W.; Hui, Z.; Zhu, N.; Lee, S. T.; Che, C. M. *Chem. Commun.* **2002**, 206.
(23) Lai, S. W.; Chan, M. C. W.; Cheung, T. C.; Peng, S. M.; Che, C. M. *Inorg. Chem.* **1999**, *38*, 4046.
(24) Lai, S. W.; Chan, M. C. W.; Cheung, K. K.; Che, C. M. *Organometallics* **1999**, *18*, 3327.
(25) Song, D.; Wu, Q.; Hook, A.; Kozin, I.; Wang, S. *Organometallics* **2001**, *20*, 4683.
(26) Newman, C. P.; Cave, G. W. V.; Wong, M. W.; Errinton, W.; Alcock, N. W.; Rourke, J. P. *J. Chem. Soc., Dalton Trans.* **2001**, 2678.
(27) Zheng, G. Y.; Rillema, D. P. *Inorg. Chem.* **1998**, *37*, 1392.
(28) Jude, H.; Bauer, J. A. K.; Connick, W. B. *Inorg. Chem.* **2002**, *41*, 2275.
(29) Cheung, T. C.; Cheung, K. K.; Peng, S. M.; Che, C. M. *J. Chem. Soc., Dalton Trans.* **1996**, 1645.
(30) DePriest, J.; Zheng, G. Y.; Goswami, N.; Eichhorn, D. M.; Woods, C.; Rillema, D. P. *Inorg. Chem.* **2000**, *39*, 1955.
(31) DePriest, J.; Zheng, G. Y.; Woods, C.; Rillema, D. P.; Mikirova, N. A.; Zandler, M. E. *Inorg. Chim. Acta* **1997**, *264*, 287.
(32) Shi, J. C.; Chao, H. Y.; Fu, W. F.; Peng, S. M.; Che, C. M. *J. Chem. Soc., Dalton Trans.* **2000**, 3128.
(33) Yam, V. W. W.; Tang, R. P. L.; Wong, K. M. C.; Lu, X. X.; Cheung, K. K.; Zhu, N. *Chem.−Eur. J.* **2002**, *8*, 4066.
(34) Neve, F.; Crispini, A.; Campagna, S. *Inorg. Chem.* **1997**, *36*, 6150.
(35) Yip, J. H. K.; Suwarno; Vital, J. J. *Inorg. Chem.* **2000**, *39*, 3537.
(36) Che, C. M.; Fu, W. F.; Lai, S. W.; Hou, Y. J.; Liu, Y. L. *Chem. Commun.* **2003**, 118.
(37) Minghetti, G.; Doppiu, A.; Stoccoro, S.; Zucca, A.; Cinellu, M. A.; Manassero, M.; Sansoni, M. *Eur. J. Inorg. Chem.* **2002**, 431.
(38) Meijer, M. D.; Kleij, A. W.; Williams, B. S.; Ellis, D.; Lutz, M.; Spek, A. L.; van Klink, G. P. M.; van Koten, G. *Organometallics* **2002**, *21*, 264.
(39) Sánchez, G.; García, J.; Meseguer, D.; Serrano, J. L.; García, L.; Pérez, J.; López, G. *J. Chem. Soc., Dalton Trans.* **2003**, 4709.
(40) Pregosin, P. S.; Wombacher, F.; Albinati, A.; Lianza, F. *J. Organomet. Chem.* **1991**, *418*, 249.
(41) Hartwell, G. E.; Lawrence, R. W.; Smas, M. J. *J. Chem. Soc., Chem. Commun.* **1970**, 912.
(42) Carty, A. J.; Hota, N. K.; Ng, T. W.; Patel, H. A.; O'Connor, T. J. *Can. J. Chem.* **1971**, *49*, 2706.

Synthesis of [Pd(bzq)Cl(PPh$_2$H)] (2). PPh$_2$H (216 μL, 1.25 mmol) was added to a pale yellow solution of [Pd(bzq)(μ-Cl)]$_2$ (0.401 g, 0.626 mmol) in CH_2Cl_2 (20 mL) at 0 °C. The dark-yellow solution obtained was filtered through Celite and evaporated to dryness. Treatment of the residue with *n*-hexane (5 mL) afforded a pale yellow solid (0.585 g, 92% yield), which contains (NMR spectroscopy) **2** and traces of other isomer (^{1}H NMR δ 9.91, 9.22, 8.73 bzq). Recrystallization from $CHCl_3$/hexane gave **2** as unique product. Yield: 0.42 g (66%). Anal. Calcd for $C_{25}ClH_{19}NPd$: C, 59.31; H, 3.78; N, 2.77. Found: C, 59.31; H, 3.72; N, 2.64. MS ES(+): *m*/*z* 470 [M − Cl]$^+$, 100%. IR (cm^{-1}): ν(P−H) 2341 (m); ν(Pd−Cl) 278 (m). ^{1}H NMR (δ, $CDCl_3$): 9.66 (s br, H^2, bzq), 8.32 (d, $^1J_{H-H}$ = 7.6 Hz, H^9, bzq), 7.95 (m, 4H, Ph/bzq), 7.77 (d, $^1J_{H-H}$ = 8.6 Hz, bzq), 7.62 (m, 3H, Ph/bzq), 7.43 (m, 7H, Ph/bzq), 7.26 (m, 1H, bzq, overlapped P-*H*), 6.62 (d, $^1J_{P-H}$ = 376 Hz, PPh$_2$*H*). Only one of the signals (at δ 6.00) for PPh$_2$*H* doublet can be observed; the other is overlapped with the signal at δ 7.26. ^{31}P{^{1}H} NMR (δ, $CDCl_3$): 20.21 (s). ^{31}P NMR (δ, $CDCl_3$): 20.2 (J_{P-H} = 376 Hz).

Synthesis of [Pt(bzq)Cl(PPh$_2$C≡CPh)] (3). A yellow suspension of [Pt(bzq)(μ-Cl)]$_2$ (0.400 g, 0.489 mmol) in CH_2Cl_2 (20 mL) was treated with PPh$_2$C≡CPh (0.280 g, 0.979 mmol), and the resulting orange solution was stirred for 30 min at room temperature. Evaporation to dryness and treatment of the oily residue with EtOH gave **3** as a yellow solid. Yield: 0.528 g (78%). Anal. Calcd for $C_{33}ClH_{23}NPPt$: C, 57.02; H, 3.33; N, 2.01. Found: C, 56.98; H, 3.30; N, 2.25. MS ES(+): *m*/*z* 659 [M − Cl]$^+$, 100%. IR (cm^{-1}): ν(C≡C) 2181 (m); ν(Pt−Cl) 296, 286 (w). ^{1}H NMR (δ, $CDCl_3$): 9.99 (m, H^2, bzq), 8.32 (d, J_{H-H} = 7.4 Hz, H^9, bzq), 7.99 (m, 4H, Ph/bzq), 7.76 (dd, $^2J_{H-H}$ = 8.5, 3.5 Hz, 1H, bzq), 7.64−7.34 (m, 16H, Ph/bzq). ^{31}P{^{1}H} NMR (δ, $CDCl_3$): −5.06 (s, $^1J_{Pt-P}$ = 4408 Hz). ^{13}C{^{1}H} NMR (δ, $CDCl_3$): 155.0 (d, $^2J_{P-C}$ = 2.4 Hz, C^{10}, bzq), 148.4 (s, $^2J_{Pt-C}$ = 27.9 Hz, C^2, bzq), 141.8 (s, $^2J_{Pt-C}$ = 24.9 Hz, C$^{13/14}$, bzq), 140.4 (d, J_{P-C} = 9.0 Hz, C$^{11/12}$, bzq), 138.4 (s, C$^{3/4}$, bzq), 133.8 (d, $^2J_{C-P}$ = 12.6 Hz, *C*$_{ortho,}$ PPh$_2$), 133.7, 133.6 (bzq), 132.3 (d, *C*$_{ortho}$, C≡CPh), 131.0 (d, $^4J_{C-P}$ = 2.4 Hz, *C*$_{para}$, PPh$_2$), 130.3 (d, J_{P-C} = 68 Hz, $^2J_{Pt-C}$ = 30 Hz, *C*$_{ipso}$, PPh$_2$), 130.1 (s, *C*$_{para}$, C≡CPh), 129.5 (d, J_{C-P} = 2.6 Hz, C^9, bzq), 129.4 (s, bzq), 128.4 (d, $^3J_{C-P}$ = 11.7 Hz, *C*$_{meta}$, PPh$_2$), 128.2 (s, *C*$_{meta}$, C≡C*Ph*), 126.7 (d, $^4J_{C-P}$ = 2.4 Hz, $^3J_{Pt-C}$ = 26 Hz, C^{12}, bzq), 123.2 (s), 122.3 (s), 121.2 (s), 121.1 (bzq, *C*$_{ipso}$ C≡CPh), 107.4 (d, $^2J_{C-P}$ = 17.0 Hz, C$_\beta$, PPh$_2$C$_\alpha$≡C$_\beta$Ph), 80.2 (d, $^1J_{C-P}$ = 113 Hz, C$_\alpha$, PPh$_2$C$_\alpha$≡C$_\beta$Ph).

Synthesis of [Pd(bzq)Cl(PPh$_2$C≡CPh)] (4). A pale-yellow suspension of [Pd(bzq)(μ-Cl)]$_2$ (0.250 g, 0.392 mmol) in CH_2Cl_2 (25 mL) was treated with PPh$_2$C≡CPh (0.223 g, 0.784 mmol), and the mixture was stirred for 2 h at room temperature. The resulting solution was filtered through Celite, and the solvent was evaporated to 2 mL to give **4** as a pale yellow solid, which was recrystallized from CH_2Cl_2/EtOH. Yield: 0.350 g (74%). Anal. Calcd for $C_{33}ClH_{23}NPPd$: C, 65.37; H, 3.82; N, 2.31. Found: C, 65.33; H, 3.73; N, 2.44. MS ES(+): *m*/*z* 570 [M − Cl]$^+$, 100%. IR (cm^{-1}): ν(C≡C) 2175 (s); ν(Pd−Cl) 301 (s). ^{1}H NMR (δ, $CDCl_3$): 9.76 (d, J_{H-H} = 4.7 Hz, H^2, bzq), 8.28 (d, J_{H-H} = 7.8 Hz, H^9, bzq), 8.01 (m, 4H, Ph/bzq), 7.73 (d, J_{H-H} = 8.6 Hz, 1H, bzq), 7.62−7.21 (m, 16H, Ph/bzq). ^{31}P{^{1}H} NMR (δ, $CDCl_3$): 13.76. ^{13}C{^{1}H} NMR (δ, $CDCl_3$): 154.3 (d, $^2J_{P-C}$ = 2.9 Hz, C^{10}, bzq), 154.2 (s, C^2, bzq), 149.4 (s, bzq), 142.6 (d, J_{P-C} = 2.2 Hz, bzq), 137.7 (s, bzq), 134.6−121.2 (bzq/Ph), 108.4 (d, $^2J_{C-P}$ = 14.0 Hz, C$_\beta$, PPh$_2$C$_\alpha$≡C$_\beta$Ph), 81.5 (d, $^1J_{C-P}$ = 97 Hz, C$_\alpha$, PPh$_2$C$_\alpha$≡C$_\beta$Ph).

Reaction of [Pt(bzq)Cl(PPh$_2$H)] (1) with PPh$_2$C≡CPh. Formation of [Pt(bzq)(PPh$_2$H)(PPh$_2$C≡CPh)]ClO$_4$ (5). To a yellow suspension of [Pt(bzq)Cl(PPh$_2$H)] **1** (0.200 g, 0.336 mmol) in acetone (10 mL), $NaClO_4 \cdot H_2O$ (0.118 g, 0.841 mmol) and PPh$_2$C≡CPh (0.096 g, 0.336 mmol) were added. After 1 h of stirring at room temperature, the solvent was evaporated to dryness and the residue was treated with CH_2Cl_2 (20 mL) and filtered through Celite. The resulting pale yellow solution was removed in vacuo, and the residue was treated with Et_2O (5 mL) to give a yellow solid. The spectroscopic data indicate the presence mainly of complex **5**, although contaminated with other products [δ 48.7, 45.41 (due to **6a**) and other unknown signals]. All attempts to obtain pure **5** from this solid were unsuccessful since **5** evolves in solution, even at low temperature, to the mixture of species **6a** + **6b**. Yield: 0.246 g (83%). Λ_M (acetone 5 × 10^{-4} M): 123 Ω^{-1} cm^2 mol^{-1}. MS ES(+): *m*/*z* 846 [M − ClO$_4$]$^+$, 100%. IR (cm^{-1}): ν(P−H) 2352 (w); ν(C≡C) 2172 (s); ν(ClO$_4^-$) 1084 (m, br), 624 (s). ^{1}H NMR (δ, $CDCl_3$): 8.7 (br), 8.58 (d, J_{H-H} = 7.7 Hz), 8.48 (d, J_{H-H} = 7.6 Hz), 7.92−7.33 (m, bzq/Ph), 6.12 (dd, $^1J_{P-H}$ = 411 Hz, $^3J_{P-H}$ = 19.5 Hz, PPh$_2$*H*). ^{31}P{^{1}H} NMR (δ, $CDCl_3$): 6.29 (s, br, $^1J_{P-Pt}$ = 1792 Hz, PPh$_2$C≡CPh trans to C), −5.08 (s, br, $^1J_{P-Pt}$ = 3798 Hz, PPh$_2$H trans to N). ^{31}P NMR (δ, $CDCl_3$): 6.46 (s, $^1J_{P-Pt}$ = 1784 Hz, PPh$_2$C≡CPh trans to C), −4.90 (d, J_{P-H} = 415 Hz).

Synthesis of [Pt(bzq)(PPh$_2$C(Ph)═C(H)PPh$_2$)]ClO$_4$ (6a, 6b). To a suspension of [Pt(bzq)Cl(PPh$_2$H)] **1** (0.100 g, 0.168 mmol) in acetone (10 mL), $NaClO_4 \cdot H_2O$ (0.070 g, 0.504 mmol) and PPh$_2$C≡CPh (0.048 g, 0.168 mmol) were added. The solution was stirred at room temperature for 3 days, and then, volatiles were removed in vacuo. The resultant residue was treated with CH_2Cl_2 (20 mL), filtered through Celite, evaporated to dryness, and treated with Et_2O to give a yellow solid. This was identified by NMR spectroscopy as a mixture of isomers **6a** and **6b** (48:52). All attempts to separate these isomers by repeated crystallizations were unsuccessful. Yield: 0.121 g (89%). Anal. Calcd for $C_{45}ClH_{34}NO_4P_2Pt$: C, 57.18; H, 3.62; N, 1.48. Found: C, 57.01; H, 3.97; N 1.36. Λ_M: 127.8 Ω^{-1} cm^2 mol^{-1}. MS ES(+): *m*/*z* 845 [M − ClO$_4$]$^+$, 100%. IR (cm^{-1}): ν(C═C) 1574 (m); ν(ClO$_4^-$) 1086 (m, br). ^{1}H NMR (δ, CD_3COCD_3): 9.11 (st, H^2, bzq), 8.87 (st, H^2, bzq), 8.80 (d, J_{H-H} = 8.1 Hz, H^9, bzq), 8.75 (d, J_{H-H} = 8.1 Hz, H^9, bzq), 8.23 (m), 7.96 (m), 7.71 (m), 7.58 (m), 7.40 (m), 7.25 (m, bzq/Ph), 6.80 (d, $^3J_{P-H}$ = 38.5 Hz), 6.77 (d, $^3J_{P-H}$ = 38.4 Hz). ^{31}P{^{1}H} NMR (δ, CD_3COCD_3): **6a**, 49.35 (s, br, $^1J_{Pt-P}$ = 3787 Hz, *P*PH$_2$C(Ph), P trans to N), 46.28 (s, br, $^1J_{P-Pt}$ = 1859 Hz, *P*Ph$_2$C(Ph), P trans to C) (molar ratio **6a**/**6b** 48:52); **6b**, 65.03 (s, br, $^1J_{Pt-P}$ = 1886 Hz, *P*Ph$_2$C(Ph), P trans to C), 33.31 (s, br, $^1J_{Pt-P}$ = 3732 Hz, C(H)*P*PH$_2$, P trans to N). ^{31}P NMR (δ, CD_3COCD_3): **6a**, 49.4 (d, $^1J_{Pt-P}$ = 3799 Hz, $^3J_{P-H}$ = 50.5 Hz, P trans to N), 46.32 (s, $^1J_{Pt-P}$ = 1874 Hz, *P*Ph$_2$C(Ph), P trans to C); **6b**, 65.03 (d, $^1J_{Pt-P}$ = 1873 Hz, $^3J_{P-H}$ = 48.8 Hz, P trans to C), 33.36 (s, $^1J_{P-Pt}$ = 3739 Hz, *P*Ph$_2$C(Ph), P trans to N).

Synthesis of [Pt(bzq)(C≡CPh)(PPh$_2$C≡CPh)] (7a, 7b). A yellow solution of [Pt(bzq)Cl(PPh$_2$C≡CPh)] **3** (0.100 g, 0.144 mmol) in $CHCl_3$ (20 mL) was treated with HC≡CPh (47.4 μL, 0.432 mmol), CuI (0.005 g, 0.026 mmol), and NEt_3 (1 mL) and stirred for 30 min at room temperature. The orange-red solution obtained was evaporated and treated with ^{i}PrOH to give **7a** as an orange solid. Starting from the same products and the same molar ratios but stirring for 10 days at room temperature, a mixture of **7a** and **7b** (50:50) was obtained. Crystals of **7b** were separated by crystallization of the mixture in acetone/hexane at −30 °C.

Data for 7a. Yield: 0.102 g (94%). Anal. Calcd for $C_{41}H_{28}NPPt$: C, 64.73; H, 3.71; N, 1.84. Found: C, 64.60; H, 4.50; N, 2.03. MS ES(+): *m*/*z* 659.5 [M − C≡CPh]$^+$, 100%. IR (cm^{-1}): ν(C≡C) 2175 (s), 2104 (m). ^{1}H NMR (δ, $CDCl_3$): 10.23 (t, $^3J_{Pt-H}$ = 30 Hz, $J_{H-H} \approx$ 3.9 Hz, H^2), 8.34 (d, J_{H-H} = 7.6 Hz, H^9), 8.02 (m, bzq/Ph), 7.77 (d, J_{H-H} = 8.6 Hz, bzq), 7.57−7.00 (bzq, Ph). ^{31}P{^{1}H}

Table 1. Crystallographic Data for **1**, **6**·CH_3COCH_3·$^1/_2CH_3(CH_2)_4CH_3$, **7b**·CH_3COCH_3, and **8**

	1	**6**·CH_3COCH_3·$^1/_2CH_3(CH_2)_4CH_3$	**7b**·CH_3COCH_3	**8**
empirical formula	$C_{25}H_{19}ClNPPt$	$C_{51}H_{47}ClNO_5P_2Pt$	$C_{44}H_{34}NOPPt$	$C_{50}H_{36}N_2P_2Pt_2$
F_w	594.92	1046.38	818.78	1116.93
T (K)	293(2)	173(1)	173(1)	293(2)
cryst syst, space group	monoclinic, $P2_1/n$	monoclinic, $P2_1/n$	triclinic, $P\bar{1}$	triclinic, $P\bar{1}$
a (Å)	12.5956(3)	15.5499(2)	8.7368(2)	8.9636(2)
b (Å)	10.0448(2)	14.5206(2)	13.2354(3)	10.7454(2)
c (Å)	17.7985(3)	20.9079(4)	16.5095(5)	17.8301(3)
α (deg)	90	90	72.1340(10)	103.6040(10)
β (deg)	110.4890(10)	110.6080(10)	84.2960(10)	103.9800(10)
γ (deg)	90	90	75.8270(10)	100.4650(10)
vol (Å^3)	2109.42(7)	4418.79(12)	1761.10(8)	951.87(4)
Z	4	4	2	1
D_{calcd} (Mg/m^3)	1.873	1.573	1.544	1.948
abs coeff (mm^{-1})	6.866	3.358	4.064	7.465
F(000)	1144	2100	812	536
θ range for data collection (deg)	3.17−27.88	3.42−26.02	1.78−27.90	2.40−27.91
no. of data/restraints/params	5020/0/266	8686/0/553	8365/0/435	4513/0/253
goodness-of-fit on F^2[a]	0.893	1.006	1.045	1.040
final R indices [$I > 2\sigma(I)$][a]	R1 = 0.0296	R1 = 0.0450	R1 = 0.0351	R1 = 0.0207
	wR2 = 0.0617	wR2 = 0.0821	wR2 = 0.0754	wR2 = 0.0471
R indices (all data)[a]	R1 = 0.0494	R1 = 0.0850	R1 = 0.0467	R1 = 0.0228
	wR2 = 0.0669	wR2 = 0.0928	wR2 = 0.0793	wR2 = 0.0480
largest diff peak and hole (e Å^{-3})	1.664 and −1.047	1.476 and −0.652	1.958 and −1.681	0.864 and −1.116

[a] $R1 = \sum(|F_o| - |F_c|)/|F_o|$; $wR2 = [\sum w(F_o^2 - F_c^2)^2/\sum wF_o^2]1/2$; goodness-of-fit $= \sum w(F_o^2 - F_c^2)^2/(N_{obs} - N_{param})]$; $w = [\sigma^2(F_o) + (g_1P)^2 + g_2P]^{-1}$; $P = [\max(F_o^2; 0) + 2F_c^2]/3$.

NMR (δ, $CDCl_3$): −8.0 (s, $^1J_{Pt-P} = 4127$ Hz). $^{13}C\{^1H\}$ NMR (δ, CD_3COCD_3): 161.6 (d, $^2J_{P-C} = 6.8$ Hz, C^{10}, bzq), 157.1 (s br, C^2, bzq), 151.1 (s, bzq), 144.4 (s, bzq), 139.0 (s, bzq), 135.4−121.0 (bzq/Ph/C_α C≡CPh), 107.7 (s, C_β, C≡CPh), 107.2 (d, $^2J_{C-P} = 16.7$ Hz, C_β, $PPh_2C_\alpha{\equiv}C_\beta Ph$), 80.7 (d, $^1J_{C-P} = 109$ Hz, C_α, $PPh_2C_\alpha{\equiv}C_\beta Ph$).

Data for 7b. Signals obtained from the mixture **7a** + **7b**. $^{31}P\{^1H\}$ NMR (δ, $CDCl_3$): 3.75 (s, $^1J_{Pt-P} = 1788$ Hz). ^1H NMR (δ, $CDCl_3$): 9.47, 9.23, 9.05, 8.74 (bzq). The rest of signals overlap with those of **7a**.

Synthesis of [Pt(bzq)(μ-PPh_2)]$_2$ (8). Method a. To a yellow suspension of [Pt(bzq)(μ-Cl)]$_2$ (0.100 g, 0.122 mmol) in acetone (15 mL), PPh_2H (42.0 μL, 0.245 mmol) and NEt_3 (1 mL) were added. After 30 min of stirring at room temperature, the yellow solid was filtered and washed with acetone (4 × 2 mL) and identified as **8**. Yield: 0.118 g (86%).

Method b. To a yellow suspension of [Pt(bzq)Cl(PPh_2H)] **1** (0.254 g, 0.426 mmol) in a mixture 1:1 of CH_2Cl_2/acetone (20 mL) was added K_2CO_3 (0.088 g, 0.640 mmol). After 5 h of stirring at room temperature, the yellow solid formed was recovered by filtration, washed with distilled water, and dried under reduced pressure (0.236 g, 96% yield). Anal. Calcd for $C_{50}H_{36}N_2P_2Pt_2$·$2H_2O$: C, 52.08; H, 3.50; N, 2.43. Found: C, 51.92; H, 2.93; N, 2.80. Its insolubility in all common solvent precluded its spectroscopic characterization.

X-ray Crystallography. Crystal data and other details of the structure analyses are presented in Table 1. Yellow (**1**, **6**, **7b**) crystals were obtained by slow diffusion of *n*-hexane into acetone (**6**, **7** at −30 °C) or chloroform (**1** at room temperature) solution of the complexes, while yellow crystals of **8** were obtained by slow reaction of complex **1** with NEt_3 in a CH_2Cl_2 solution at room temperature. For complex **6**, one molecule of acetone and half a molecule of *n*-hexane was found in the asymmetric unit, and for complex **7b**, one molecule of acetone was found in the asymmetric unit. X-ray intensity data were collected with a NONIUS κCCD area-detector diffractometer using graphite-monochromated Mo Kα radiation. Images were processed using the DENZO and SCALEPACK suite of programs,[43] carrying out the absorption correction at this point for complex **8**. For the rest of complexes, the absorption correction was performed using SORTAV.[44] All the structures were solved by Patterson and Fourier methods using the DIRDIF92 program[45] and refined by full-matrix least squares on F^2 with SHELXL-97.[46] All non-hydrogen atoms were assigned anisotropic displacement parameters, and all hydrogen atoms were constrained to idealized geometries fixing isotropic displacement parameters of 1.2 times the U_{iso} value of their attached carbon for the phenyl and CH_2 hydrogens and 1.5 for the methyl groups. To establish the identities of the C and N atoms of the 7,8-benzoquinoline ligand, each structure (except **8**) was refined in three different ways (with the identities of the C and N in one position, with the element types reversed, and with 50/50 hybrid scattering factor at each of the affected atomics sites). Examination of the ΔMSDA values for bonds involving these atoms revealed the correct assignments[47,48] (Supporting Information). For complexes **1**, **6**, and **7b**, some residual peaks higher than 1 e Å^{-3} were observed close to their respective platinum atoms but with no chemical meaning.

Results and Discussion

Synthesis and Characterization. The synthesis of the platinum and palladium complexes is shown in Scheme 1. Bridge cleavage of [M(bzq)(μ-Cl)]$_2$ (M = Pt, Pd; bzqH = benzoquinoline ligand) with 2 equiv of PPh_2H or $PPh_2C{\equiv}CPh$ in CH_2Cl_2 affords the neutral mononuclear yellow complexes

(43) Otwinowski, Z.; Minor, W. In *Methods in Enzymology*; Carter, C. V., Jr., Sweet, R. M., Eds.; Academic Press: New York, 1997; Vol. 276A, p 307.
(44) Blessing, R. H. *Acta Crystallogr.* **1995**, *A51*, 33.
(45) Beursken, P. T.; Beursken, G.; Bosman, W. P.; de Gelder, R.; García-Granda, S.; Gould, R. O.; Smith, J. M. M.; Smykalla, C. *The DIRDIF92 Program System*; Technical Report of the Crystallography Laboratory; University of Nijmegen: Nijmegen, The Netherlands, 1992.
(46) Sheldrick, G. M. *SHELX-97, a Program for the Refinement of Crystal Structures*; University of Göttingen: Göttingen, Germany, 1997.
(47) Hirshfeld, F. L. *Acta Crystallogr., Sect. A* **1976**, *32*, 239.
(48) Displacement parameter analysis was done using the program PLATON: Speck, A. L. *Acta Crystallogr., Sect. A* **1990**, *46*, C34.

Scheme 1

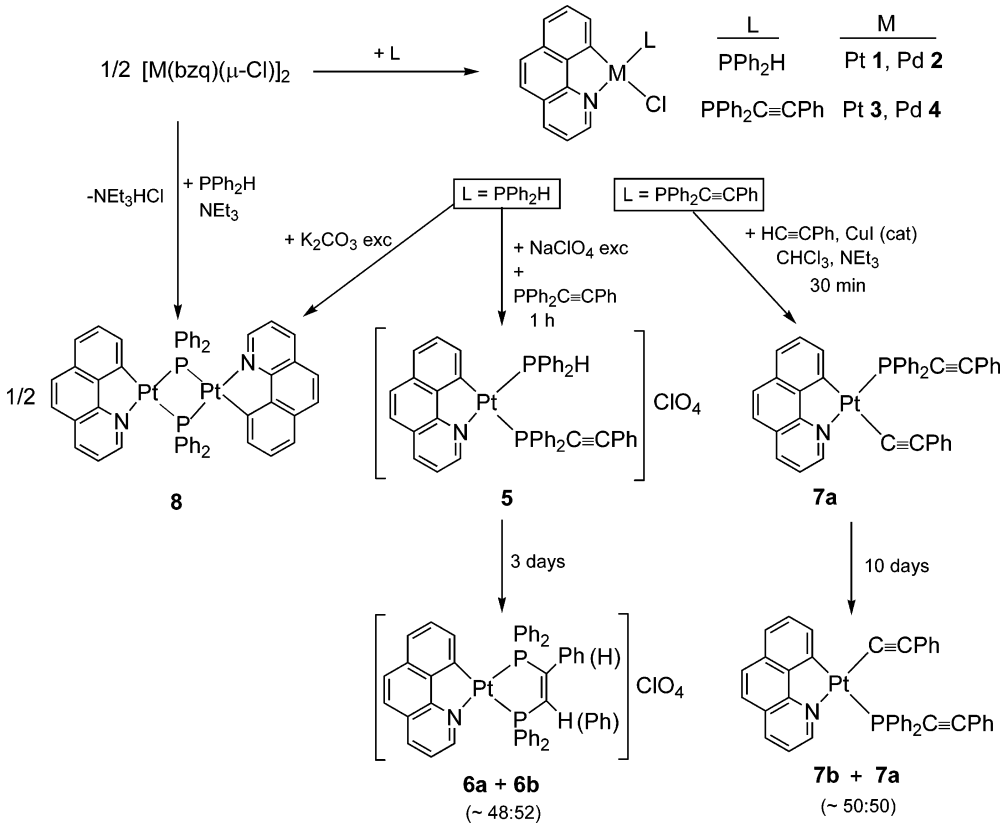

[M(bzq)Cl(L)] (L = PPh_2H, M = Pt **1**, Pd **2**; L = $PPh_2C{\equiv}CPh$, M = Pt **3**, Pd **4**). Their spectroscopic data and the structural analysis of complex **1** (see below) confirm the formation of the isomers with the nitrogen and the P atoms in trans position. The preferential formation of this isomer is in agreement with the so-called *transphobia* effect[49,50] and the *antisymbiotic* effect,[51] which show the tendency to locate the softer ligands (C_{sp^2} and P) in cis position. Infrared spectra show the characteristic absorption of the phosphine ligands, ν(P−H) vibration (2364 cm^{-1} **1**, 2341 cm^{-1} **2**) and a weak absorption in the expected range for the P-coordinated alkynylphosphine (2181 cm^{-1} **3**, 2175 cm^{-1} **4**). The $^{31}P\{^1H\}$ NMR spectra of **1**−**4** contain one sharp singlet, with ^{195}Pt satellites in **1** and **3**. In accordance with the isomer shown in Scheme 1, the high value of the $^1J_{Pt-P}$ (4149 Hz **1**, 4408 Hz **3**) is consistent with the trans disposition of the phosphine ligands with the N atom, and it is in agreement with the lower trans influence of nitrogen in relation to orthometalated carbon. Similar values have been reported in related complexes with bzq and phosphine ligands.[30,40] As expected, the proton coupled ^{31}P NMR spectra of **1** and **2** exhibit a doublet due to phosphorus−hydrogen coupling ($^1J_{P-H}$ is 414 Hz **1**, 376 Hz **2**) with ^{195}Pt satellites. The proton NMR spectra (see Chart 1 for labeling) exhibit two characteristic[15−17] low-field signals in the range 9.99−9.66 (ppm) and 8.35−8.28 (ppm) due to the H^2 and H^9 protons of the bzq ligand, respectively.

Chart 1

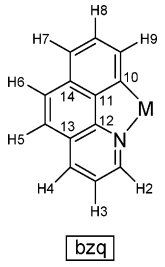

In complex **1**, the value of $^3J_{Pt-H^2}$ (26 Hz) is similar to those observed in related Pt(II) complexes.[15−17] In addition, complexes **1** and **2** display the P−H resonance as a doublet, with Pt satellites in the case of **1**, in the expected region (δ 6.81 **1**, 6.62 **2**). The $^{13}C\{^1H\}$ NMR spectra of **1**, **3**, and **4** show the expected resonances for the bzq ligand in addition to those of PPh_2H or $PPh_2C{\equiv}CPh$ ligands. Some of the signals are tentatively assigned on the basis of the $^{195}Pt-^{13}C$ (**1**, **3**) and $^{31}P-^{13}C$ coupling constants and according to the signals observed in related Pt(II) complexes[15−17](see Experimental Section). In complexes **3** and **4**, the C_α and C_β acetylenic carbons appear (δ C_α/C_β 80.2/107.4 **3**, 81.5/108.4 **4**) as doublets, with coupling constants J_{P-C} of 113 and 17 Hz (**3**), 97 and 14 Hz (**4**), respectively. Although both signals are upfield-shifted with regard to those of the free $PPh_2C{\equiv}CPh$ (δ C_α /C_β 86.5/109.4), the chemical shift difference [$\Delta\delta(C_\beta - C_\alpha)$ 27.2 **3**, 26.9 **4**], which has been previously related to the triple-bond polarization,[52,53] is slightly higher than in $PPh_2C{\equiv}CPh$.

We also decided to examine the preparation of a platinum complex containing the bzq ligand and two different

(49) Vicente, J.; Abad, J. A.; Martínez-Viviente, E.; Jones, P. G. *Organometallics* **2002**, *21*, 4454.
(50) Vicente, J.; Arcas, J. A.; Farkland, A. D.; Ramírez de Arellano, M. C. *Chem.—Eur. J.* **1999**, *5*, 3066.
(51) Pearson, R. G. *Inorg. Chem.* **1973**, *2*, 163.

coordinated phosphorus ligands, PPh_2H and $PPh_2C{\equiv}CPh$. This kind of system could be of interest, taking into account the precedents on P−H activation bond by addition of a secondary phosphine to a coordinated alkynylphosphine.[54,55] Treatment of [Pt(bzq)Cl($PPh_2C{\equiv}CPh$)] **3** with 1 equiv of PPh_2H in CH_2Cl_2 immediately resulted in the exchange of phosphine ligands yielding complex [Pt(bzq)Cl(PPh_2H)] **1**. When the reaction was carried out in the presence of $NaClO_4$, an equimolar mixture of **1** and of the isomers **6a** and **6b** was obtained, and in the presence of a stoichiometric amount of $AgClO_4$, a mixture of species (which includes in this case the complex **5**) was also obtained. As an alternative route, we used [Pt(bzq)Cl(PPh_2H)] **1** as precursor (Scheme 1). Thus, treatment of **1** with $PPh_2C{\equiv}CPh$ in the presence of an excess of $NaClO_4$ gave a pale yellow solid identified as [Pt(bzq)(PPh_2H)($PPh_2C{\equiv}CPh$)](ClO_4) **5**, contaminated with small amounts of **6a** and small amounts of other unknown species. Attempts to purify **5** by recrystallization in several solvents were unsuccessful, since this complex **5** evolves in solution, even at low temperature, to the asymmetric diphosphine complex [Pt(bzq)($PPh_2C(Ph){=}C(H)PPh_2$)]ClO_4 **6**. In fact, the synthetic strategy for making complex **6** involves the prolongated reaction of **1** with $PPh_2C{\equiv}CPh$ at room temperature in the presence of $NaClO_4$ (excess) for 3 days. Complex **6** was obtained as a pale yellow solid in high yield (90%) and identified by NMR spectroscopy as an equimolecular mixture of isomers **6a** and **6b** of the *cis*-1,2-diphosphinoalk-1-ene complex [Pt(bzq)($PPh_2C(Ph){=}C(H)PPh_2$)]ClO_4 **6**. Formally, **6** is generated by addition of a P−H bond to the coordinated $PPh_2C{\equiv}CPh$ ligand and has been confirmed by an X-ray diffraction study.

Both complexes (**5** and **6**) behave as 1:1 electrolytes,[56] and **6** shows the molecular peak $[M - ClO_4]^+$ as the parent peak. Their spectroscopic data are very different. The most remarkable fact is the absence of the ν(P−H) and ν(C≡C) absorptions in the IR spectrum of **6**, which are in the expected range in complex **5** (2352 and 2172 cm^{-1}). In **6**, a medium band at ca. 1574 cm^{-1} was in the expected range for the ν(C=C) stretch from the diphosphine-alkene. The presence of the chelated diphosphine is clearly inferred from the $^{31}P\{^1H\}$ NMR spectra. Thus, complex **5** shows two broad singlets at δ 6.29 and −5.08 flanked by platinum satellites. The low-frequency signal (δ −5.08), which exhibits a large $^{195}Pt-P$ coupling constant of 3798 Hz and splits into a doublet due to P−H coupling (415 Hz) under off conditions, is attributed to the phosphorus atom of the PPh_2H ligand trans to N. The signal at δ 6.29 assigned to the $PPh_2C{\equiv}CPh$ ligand shows smaller $^1J_{Pt-P}$ coupling (1792 Hz) in accordance with the higher trans influence of the metalated carbon. However, the $^{31}P\{^1H\}$ NMR spectrum (CD_3COCD_3) of **6** exhibits two pairs of broad singlet signals with platinum satellites in the low-field region indicating the presence of a mixture of two isomers (**6a** and **6b**) in a ca. molar ratio of 48:52, which cannot be separated by crystallization procedures. A similar mixture of isomers is observed even in microcrystalline samples obtained from slow crystallization of acetone/*n*-hexane at low temperature. The assignment of each signal, shown in Scheme 2, was made on the basis of their coupling constants, their intensity ratio, and the analysis of their ^{31}P NMR spectrum, which shows that the signals at δ 65.03 and 49.35 split into doublet resonances by P−H coupling ($^3J_{P-H} \sim 50$ Hz) being therefore attributed to phosphorus atoms trans to the vinylic proton in each isomer. The proton spectra of **5** and **6** are also different. Whereas complex **5** shows a doublet of doublets centered at δ 6.12 ($^1J_{P-H}$ 411 Hz, $^3J_{P-H}$ 19.5 Hz) due to the P−H proton, the ^1H NMR spectrum of **6** indicates the presence of both isomers **6a** and **6b** (∼1:1), exhibiting two doublet resonances of similar intensity at δ 6.80 and 6.77 ($^3J_{P-H}$ 38.5, 38.4 Hz) assigned to each vinyl proton on each isomer.

Scheme 2

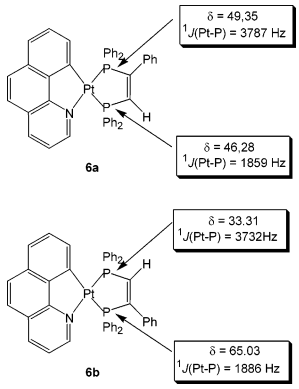

Alkynyl complexes are often obtained by a CuI-catalyzed chloride-to-alkyne metathesis.[22,57−59] With the aim of incorporating acetylide units to modulate the luminescent properties, we have examined the reaction of [Pt(bzq)Cl($PPh_2C{\equiv}CPh$)] **3** with a mixture of $HC{\equiv}CPh$, NEt_3, and CuI in $CHCl_3$ at room temperature (see Experimental Section). With a short time of reaction (30 min), the reaction takes place initially with retention of the geometry of the precursors affording the alkynyl derivative [Pt(bzq)($C{\equiv}CPh$)($PPh_2C{\equiv}CPh$)] **7a** (P trans to N). However, monitoring of the reaction for longer time indicates the slow isomerization of **7a** to **7b** yielding a final mixture of ca.1:1 molar ratio after 10 days of stirring. The identity of **7a** has been confirmed by satisfactory analyses, ^1H, $^{31}P\{^1H\}$, and $^{13}C\{^1H\}$ NMR spectroscopies, IR, and ES(+) MS, and for isomer **7b**, X-ray crystallography (see below) on a suitable crystal obtained from the mixture **7a** + **7b** dissolved in CH_3COCH_3 and layered with hexane at −30 °C. The IR spectrum of **7a** confirms the presence of P-coordinated $PPh_2C{\equiv}CPh$ [$\nu(C{\equiv}C)$ 2175 cm^{-1}] and ter-

(52) Carty, A. J. *Pure Appl. Chem.* **1982**, *54*, 113.
(53) Louattani, E.; Lledós, A.; Suades, J.; Alvarez-Larena, A.; Piniella, J. F. *Organometallics* **1995**, *14*, 1053.
(54) Carty, A. J.; Johnson, D. K.; Jacobson, S. E. *J. Am. Chem. Soc.* **1979**, *101*, 5612.
(55) Johnson, D. K.; Rukachaisirikul, T.; Sun, Y.; Taylor, N. J.; Canty, A. J.; Carty, A. J. *Inorg. Chem.* **1993**, *32*, 5544.
(56) Geary, W. J. *Coord. Chem. Rev.* **1971**, *7*, 81.
(57) Janka, M.; Anderson, G. K.; Rath, N. P. *Organometallics* **2004**, *23*, 4382.
(58) D'Amato, R.; Fratoddi, I.; Cappotto, A.; Altamura, P.; Delfini, M.; Bianchetti, C.; Bolasco, A.; Polzonetti, G.; Russo, M. V. *Organometallics* **2004**, *23*, 2860.
(59) Takahashi, S.; Kuroyama, Y.; Sonogashira, K.; Hagihara, N. *Synthesis* **1980**, 627.

Table 2. Selected Bond [Å] and Angles (deg) for [Pt(bzq)Cl(PPh_2H)] **1**

Pt(1)−N(1)	2.090(4)	Pt(1)−P(1)	2.2097(12)
Pt(1)−C(1)	2.014(5)	Pt(1)−Cl(1)	2.3869(12)
N(1)−Pt(1)−C(1)	82.33(19)	P(1)−Pt(1)−Cl(1)	89.37(5)
N(1)−Pt(1)−P(1)	177.56(11)	C(14)−P(1)−C(20)	106.6(2)
C(1)−Pt(1)−Cl(1)	174.33(15)	C(14)−P(1)−H(1)	101(2)
N(1)−Pt(1)−Cl(1)	92.15(12)	C(20)−P(1)−H(1)	100(2)
C(1)−Pt(1)−P(1)	96.11(15)		

Table 3. Selected Bond [Å] and Angles (deg) for [Pt(bzq)($PPh_2C(Ph)$═$C(H)PPh_2$]ClO_4·CH_3COCH_3·$^1/_2CH_3(CH_2)_4CH_3$ **6**·CH_3COCH_3·$^1/_2CH_3(CH_2)_4CH_3$[a]

Pt(1)−N(1a)	2.099(5)	Pt(1)−P(1)	2.2598(15)
Pt(1)−C(43a)	2.084(5)	Pt(1)−P(2)	2.2672(15)
P(2)−C(2)	1.816(6)	C(1)−C(2)	1.338(7)
P(1)−C(1)	1.818(6)	C(2)−H(2)	0.9300
N(1a)−Pt(1)−C(43a)	80.01(19)	P(1)−Pt(1)−P(2)	85.18(5)
N(1a)−Pt(1)−P(2)	98.74(13)	Pt(1)−P(2)−C(2)	107.99(19)
C(43a)−Pt(1)−P(1)	96.17(14)	Pt(1)−P(1)−C(1)	110.03(18)
P(2)−C(2)−C(1)	120.4(4)	P(1)−C(1)−C(2)	116.2(4)
P(2)−C(2)−C(1)	120.4(4)	C(2)−C(1)−P(1)	116.2(4)
P(1)−C(1)−C(3)	120.5(4)	P(2)−C(2)−H(2)	119.8
C(2)−C(1)−P(1)	116.2(4)	H(2)−C(2)−C(1)	119.8
C(2)−C(1)−C(3)	123.0(5)		

[a] Symmetry transformations used to generate equivalent atoms are #1 $-x, -y, -z$; #2 $x - 1/2, -y + 1/2, z - 1/2$; #3 $x + 1/2, -y + 1/2, z + 1/2$; #4 $-x + 3/2, y + 1/2, -z + 1/2$; #5 $-x + 3/2, y - 1/2, -z + 1/2$.

Table 4. Selected Bond [Å] and Angles (deg) for [Pt(bzq)($C\equiv CPh$)($PPh_2C\equiv CPh$)]·CH_3COCH_3 **7b**·CH_3COCH_3

Pt(1)−C(1)	1.965(4)	Pt(1)−P(1)	2.3162(10)
Pt(1)−C(31)	2.061(4)	C(1)−C(2)	1.203(6)
P(2)−N(1)	2.111(3)		
C(1)−Pt(1)−C(31)	90.34(15)	C(1)−Pt(1)−P(1)	86.11(11)
C(1)−Pt(1)−N(1)	169.27(14)	C(31)−Pt(1)−P(1)	173.86(11)
C(31)−Pt(1)−N(1)	79.88(14)	N(1)−Pt(1)−P(1)	104.01(9)

minal C≡CPh [ν(C≡C) 2104 cm^{-1}] ligands, respectively. The most remarkable difference between the isomers **7a** and **7b** is seen in the $^{31}P\{^1H\}$ NMR spectra. A singlet at δ −8.0 is due to **7a** ($^1J_{Pt-P}$ 4127 Hz), whereas the singlet at δ 3.75 ($^1J_{Pt-P}$ 1788 Hz), observed in the mixture of both species in solution, is attributed to **7b**.

The dinuclear phosphido-bridge complex [Pt(bzq)(μ-PPh_2)]$_2$ **8** is obtained in a single step by treatment of [Pt(bzq)(μ-Cl)]$_2$ with 2 equiv of PPh_2H in the presence of excess of NEt_3 or alternatively, as is shown in Scheme 1, by treatment of [Pt(bzq)Cl(PPh_2H)] **1** in CH_2Cl_2 with excess of K_2CO_3 as deprotonating agent (see Experimental Section). Its extreme insolubility precluded its spectroscopic characterization. However, the molecular structure of **8** could be determined by X-ray diffraction (see below) on crystals obtained as described in the Experimental Section.

X-ray Crystal Structures. Molecular structures of **1**, **6**, **7b**, and **8** were confirmed by X-ray diffraction. Selected bond distances and angles are shown in Tables 2−5, and the perspective drawing of the complexes are depicted in Figures 1−4. The structural analyses of **1** confirms the relative cis position of the metalated carbon atom and the P atom of the PPh_2H ligand. The preference for this cis arrangement (C, P), which has been previously observed in other mononuclear cyclometalated phosphine platinum complexes,[38,50] is probably associated with the destabilization inherent to isomers placing ligands with high trans influence in mutually trans position. In fact, the driving force behind the isomerization of **7a** to **7b** can be rationalized on the same basis. Initial alkynyl-chloride exchange on **3** produces **7a** as the kinetic product but, due to the fact that the C≡CPh group displays a higher trans influence than the $PPh_2C\equiv CPh$ ligand, this isomer **7a** evolves slowly, in this case, to a final equimolar mixture of **7a** and **7b**.

Table 5. Selected Bond [Å] and Angles (deg) for [Pt(bzq)(μ-PPh_2)]$_2$ **8**

Pt(1)−N(1)	2.091(3)	Pt(1)−P(1[a])	2.2982(8)
Pt(1)−C(1)	2.092(3)	Pt(1)−P(1)	2.3108(8)
Pt···Pt	3.601		
N(1)−Pt(1)−C(1)	80.01(12)	C(1)−Pt(1)−P(1)	173.85(8)
N(1)−Pt(1)−P(1)	101.13(9)	N(1)−Pt(1)−P(1[a])	175.27(8)
C(1)−Pt(1)−P(1[a])	102.07(9)	P(1[a])−Pt(1)−P(1)	77.25(3)
Pt(1[a])−P(1)−Pt(1)	102.75(3)		

[a] Symmetry transformations used to generate equivalent atoms are #1 $-x, -y + 2, -z$.

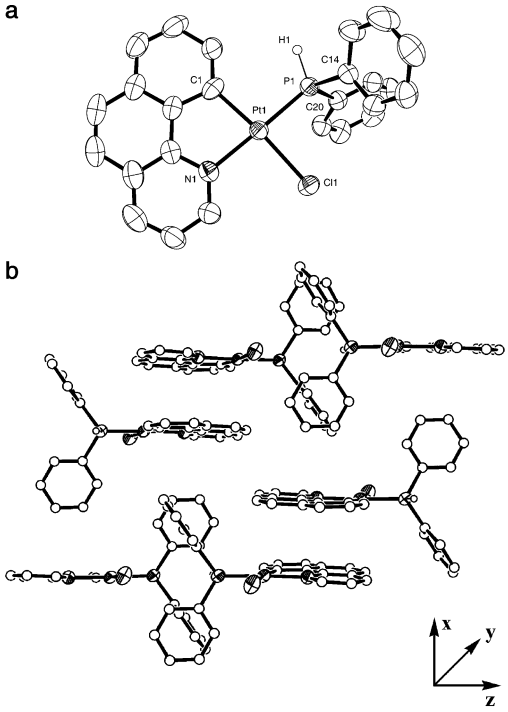

Figure 1. (a) Molecular structure of [Pt(bzq)Cl(PPh_2H)] **1**. Ellipsoids are drawn at the 50% probability. (b) Packing diagram for **1**.

As is observed in Figure 2, in complex **7b** the P atom of the $PPh_2C\equiv CPh$ ligand is now located trans to the metalated carbon atom. In complex **6** (Figure 3), which confirms the formation of the new diphosphine-alkene ligand, the C and N are found to be crystallographically indistinguishable (see Experimental Section and Supporting Information). Both atoms randomly occupy the same site through the crystal lattice giving rise to averaged Pt−C and Pt−N bond lengths. The binuclear complex **8** is stabilized by a double phosphide bridge (Figure 4) and crystallizes as the more symmetrical antiisomer as observed previously for other μ-phosphide dimers.[60−65]

(60) Falvello, L. R.; Forniés, J.; Gómez, J.; Lalinde, E.; Martín, A.; Moreno, M. T.; Sacristán, J. *Chem.—Eur. J.* **1999**, *5*, 474.

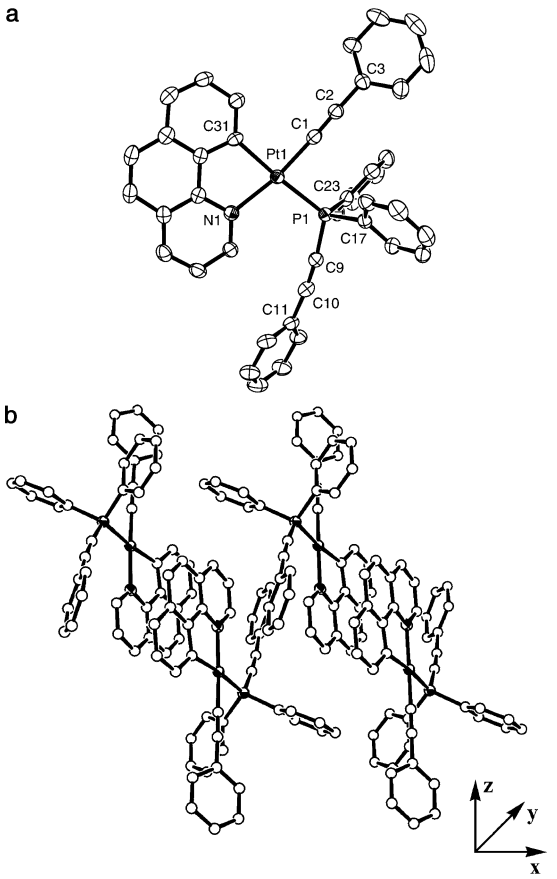

Figure 2. (a) Molecular structure of [Pt(bzq)(C≡CPh)(PPh_2C≡CPh)] **7b**. Ellipsoids are drawn at the 50% probability. (b) Packing diagram for **7b**.

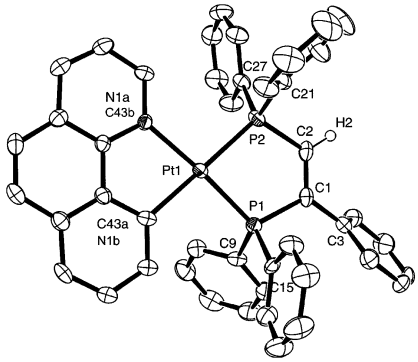

Figure 3. Molecular structure of the cation in [Pt(bzq)(PPh_2C(Ph)═C(H)PPh_2)]ClO_4 **6**. Ellipsoids are drawn at the 50% probability.

In all complexes, the platinum environments are approximately square planar with the "Pt(C^N)" moieties essentially planar and bond parameters comparable to those observed in related complexes. The narrow NPtC bite angle [range 79.88(4)−82.33(19)°] is comparable to those found in other orthoplatinated complexes.[15−17,30,31,37,38,66−68] The

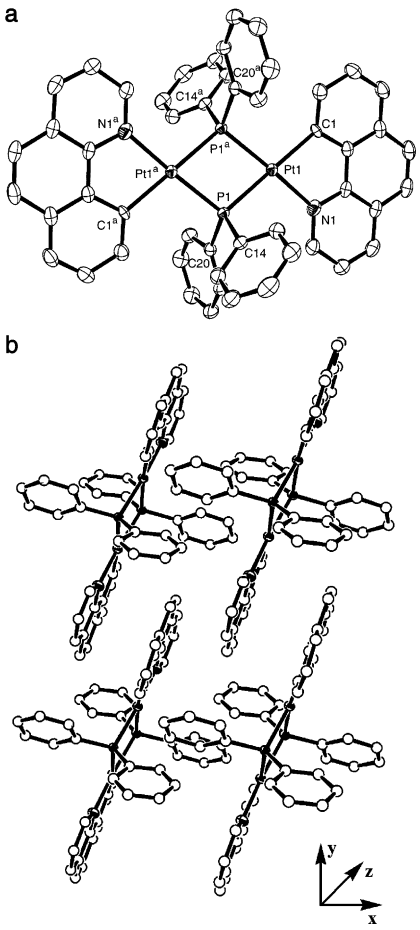

Figure 4. (a) View of the molecular structure [Pt(bzq)(μ-PPh_2)]$_2$ **8**. (b) Packing lattice for **8**.

Pt−C metalated/Pt−N bond distances in **1** and **7b** [2.014(5)/2.090(4) Å **1**; 2.061(4)/2.111(3) Å **7b**] are found to vary in accordance with the trans influence of the two ligands occupying the other two sites. For complex **6**, in which the C and N atoms are crystallographically indistinguishable [2.084(5)/2.099(5) Å **6**], and for the binuclear bis(μ-phosphido) platinum complex **8** [2.092(3)/2.091(3) Å], these distances are identical within experimental error. By comparison, the Pt−C and Pt−N bond distances of the homoleptic derivative *cis*-[Pt(bzq)$_2$] are 1.999(12), 1.976(9) Å/2.153(8), 2.149(9) Å.[17]

In **8**, the central Pt_2P_2 core is almost planar, exhibiting angles at the Pt center [P(1)−Pt(1)−P(1a) 77.25(3)°] and at the phosphorus atom [Pt(1)−P(1)−Pt(1a) 102.75(3)°] comparable to those found in other phosphide-bridge platinum(II) dimers without metal−metal bonds[60−65] (Pt···Pt 3.601 Å). It is noteworthy that the Pt−P bonds trans to Pt−C bond are longer than Pt−P bonds trans to a Pt−N bond [Pt(1)−P(1) 2.3162(10) Å **7b** vs Pt(1)−P(1) 2.2097(12) Å **1**], which could be attributed, again, to the greater trans influence of an anionic carbon center over that of a neutral iminic nitrogen atom.

In the molecular packing of complex **1** (Figure 1b), the molecules pack as head-to-tail dimers along the *x* axes related by a center of inversion, with the pyridinic and the metalated rings of both bzq ligands almost eclipsed. However, the interplanar separation (3.85 Å) is long, implying an almost

(61) Kourkine, I. V.; Chapman, M. B.; Glueck, D. S.; Eichele, K.; Wasylishen, R. E.; Yap, G. P. A.; Liable-Sands, L. M.; Rheingold, A. L. *Inorg. Chem.* **1996**, *35*, 1478.
(62) Bleeke, J. R.; Rhode, A. M.; Robinson, K. D. *Organometallics* **1995**, *14*, 1674.
(63) Brown, M. P.; Buckett, J.; Harding, M. M.; Lynden-Bell, R. M.; Mays, M. J.; Woulfe, K. W. *J. Chem. Soc., Dalton Trans.* **1991**, 3097.
(64) Leoni, P.; Manetti, S.; Pasquali, M. *Inorg. Chem.* **1995**, *34*, 749.
(65) Forniés, J.; Fortuño, C.; Navarro, R.; Martínez, F.; Welch, A. J. *J. Organomet. Chem.* **1990**, *394*, 643.

Table 6. Absorption Data (5×10^{-5} M Solutions) for Complexes **1**−**4**, **6**, and **7a**

compd	absorption/nm ($10^3\,\epsilon$/M^{-1} cm^{-1})
1	220 sh (16.4), 240 (63.0), 255 sh (54.1), 305 (27.7), 322 sh (18.5), 395 (4.9), 410 (5.6) (CH_2Cl_2)
	226 (41.2), 255 sh (37.6), 300 (12.8), 319 sh (7.9), 395 (2.13), 405 (2.1) (acetonitrile)
	212 (14), 319 sh (2.5), 326 (6.6), 338 sh (4.3), 390 (2.0), 402 (2.4) (acetone)
2	241 (65.3), 278 sh (31.2), 290 (35.8), 310 sh (19.1), 347 (4.8), 362 (5.8), 382 (7.1) (CH_2Cl_2)
	215 sh (47.6), 229 (52.3), 239 sh (44.4), 277 sh (16.4), 289 (18.9), 310 sh (10.2), 345 (4.2), 362 (4.1), 385 (3.6) (acetonitrile)
	211 (13.4), 326 (2.9), 345 (2.0), 365 (2.4), 382 (2.7) (acetone)
3	220 sh (15.4), 242 (63.8), 267 (56.3), 306 (30.2), 400 (4.9), 414 (5.3) (CH_2Cl_2)
	218 sh (43.7), 234 (55.7), 257 sh (42.9), 303 (16.2), 400 (2.8) (acetonitrile)
	211 (12.7), 326 (6.5), 342 sh (3.9), 375 (1.7), 401 (2.2), 414 (2.3) (acetone)
4	241 (67.3), 274 sh (58.3), 290 sh (42.2), 312 sh (23.2), 345 (7.7), 367 (7.7), 385 (7.8) (CH_2Cl_2)
	234 (58.0), 268 sh (34.4), 290 sh (21.1), 314 sh (9.7), 344 (3.8), 364 (3.2), 383 (3.2) (acetonitrile)
	211 (11.5), 319 (2.0), 327 (4.7), 345 (3.2), 365 (2.7), 387 (2.7) (acetone)
6	258 (60.1), 287 (41.1), 298 (39.0), 343 (4.34), 382 (4.34), 403 (4.7) (CH_2Cl_2)
	327 (8.3), 341 sh (4.9), 380 (4.2), 396 (4.5) (acetone)
	198 (58.0), 213 (67.3), 253 (63.1), 283 (40.3), 293 (37.9), 340 (4.1), 380 (4.1), 400 (4.1) (acetonitrile)
7a	220 sh (15.8), 242 (63.1), 270 (56.3), 306 sh (30.5), 347 sh (17.7), 380 sh (5.1), 425 (5.0) (CH_2Cl_2)
	212 (68.1), 240 (70.4), 265 (62.3), 310 (33.6), 333 (25.0), 346 (21.5), 380 (7.7), 420 (4.7) (acetonitrile)
	211 (12.6), 319 (5.4), 333 (13.8), 347 sh (11.8), 380 (3.8), 420 (2.7) (acetone)

negligible $\pi-\pi$ interaction.[20−24] In complex **7b**, the molecules are also packed in dimers along the *x* axes through $\pi\cdots\pi$ interactions between the aromatic benzoquinolate rings, which are parallel and displaced ca. 4 Å (defined as the distance between the centers of the pyridinic and cyclometalated rings of related bzq ligands) (Figure 2b). In this complex, there is a close interaction between the piridinic and central fused rings (3.56 Å) but a large Pt···Pt separation of 7.233 Å. The crystal packing of the dimeric complex **8** is shown in Figure 4b. The presence of two bzq ligands in each molecule facilitates the existence of $\pi\cdots\pi$ stacking interactions between different molecules of adjacent columns running along the *x* axes, yielding layers. In this case, the bzq ligands of the adjacent molecules of different columns are also parallel and slightly displaced (3.60 Å, defined as above). The pyridinic and the central rings are almost eclipsed but with a very weak intermolecular π-stacking (∼3.75 Å).

Optical Properties. Absorption Spectra. The UV−vis absorption data of complexes **1**−**7** are summarized in Table 6. All complexes show several high-energy intense absorptions in the range 211−347 nm (CH_2Cl_2, $\epsilon > 10^4$ M^{-1} cm^{-1}) that are assigned to metal-perturbed ligand-centered transitions (^{1}IL $\pi \rightarrow \pi^*$) of the bzq ligand and/or coligands.[27,30,31] They also exhibit two less intense transitions at lower energy

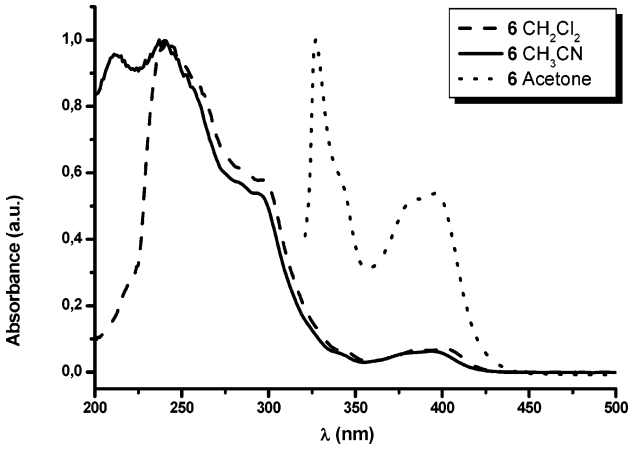

Figure 5. Normalized UV−vis absorption spectra of **6** in several solvents at 298 K.

(CH_2Cl_2, range 380−425 nm, ϵ (4.2−7.8) $\times 10^3$ M^{-1} cm^{-1}) which are tentatively assigned as metal-to-ligand charge-transfer transitions from the dπ filled metal orbitals to a vacant π^*(C^N) orbital (MLCT) [(d) $\pi \rightarrow \pi^*$(C^N)] in agreement with previous assignments in analogous platinum and palladium(II) complexes based on cyclometalated C^N aromatic rings,[14,17,22,27,30,31,68,69] These low-energy bands do not exhibit a remarkable solvatochromism (Table 6 and see Figure 5 for complex **6**) but are significantly red-shifted in the platinum complexes in relation to those in the analogous palladium systems (382 nm **2** vs 410 nm **1**; 385 nm **4** vs 414 nm **3**), which is indicative of their metal-to-ligand charge-transfer character.[25,34,70] For **6**, the low-energy absorptions are slightly blue-shifted probably due to its cationic nature, which will tend to decrease the energy of the dπ(Pt) orbitals, consequently raising the energy of the transition. The absorption profile of complex **7a** in the low-energy region shows a continuum from 345 to 425 nm (CH_2Cl_2)-420 (acetonitrile or acetone) with a tail to 450 nm. This result could be due to an overlapping of the MLCT transition with some metal-perturbed intraligand $\pi\pi^*$(C≡CR) character or even with some contribution of ligand-to-ligand charge-transfer from the acetylide ligand to bzq ligand (LL'CT).

Emission Spectra. The palladium complexes **2** and **4** are not luminescent. All platinum complexes, except **8** at room temperature, which emits very weakly, and **7a**, are intensively emissive in both the solid state and in CH_2Cl_2 glass. None of the compounds emits in solution at 298 K, most likely because of nonradiative deactivation by facile solvent/complex interaction in fluid state at room temperature. The results of the measurements in solid (298, 77 K) and glass are summarized in Table 7. Representative emission spectra are shown in Figures 6, 7, and 8. As can be observed in

(66) Hoogervost, J. W.; Elsevier, C. J.; Lutz, M.; Spek, A. *Organometallics* **2001**, *20*, 4437.
(67) McAdam, C. J.; Blackie, E. J.; Morgan, J. L.; Mole, S. A.; Robinson, B. H.; Simpson, J. *J. Chem. Soc., Dalton Trans.* **2001**, 2362.
(68) Ghedini, M.; Pucci, D.; Crispini, A.; Barberio, G. *Organometallics* **1999**, *18*, 2116.
(69) Balashev, K. P.; Puzyk, M. V.; Kotlyar, V. S.; Kulikova, M. V. *Coord. Chem. Rev.* **1997**, *159*, 109.
(70) Pérez, S.; López, C.; Caubet, A.; Bosque, R.; Solans, X.; Bardía, M. F.; Roig, A.; Molins, E. *Organometallics* **2004**, *23*, 224 and references therein.

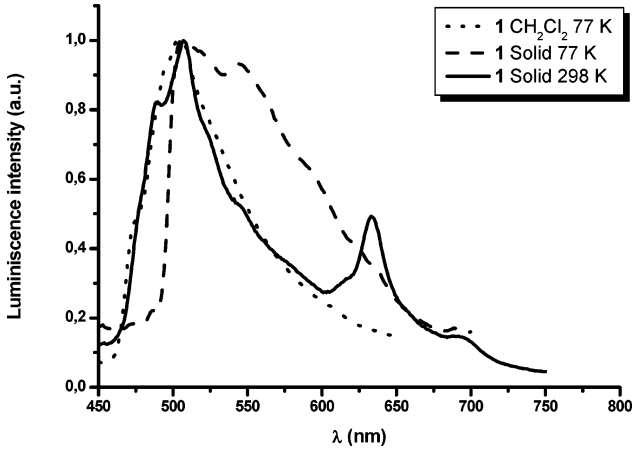

Figure 6. Normalized emission spectra of **1** in solid state at 298 K (−, λ_{ex} 400), at 77 K (- - -, λ_{ex} 400), and in CH_2Cl_2 glass at 77 K (···, λ_{ex} 390).

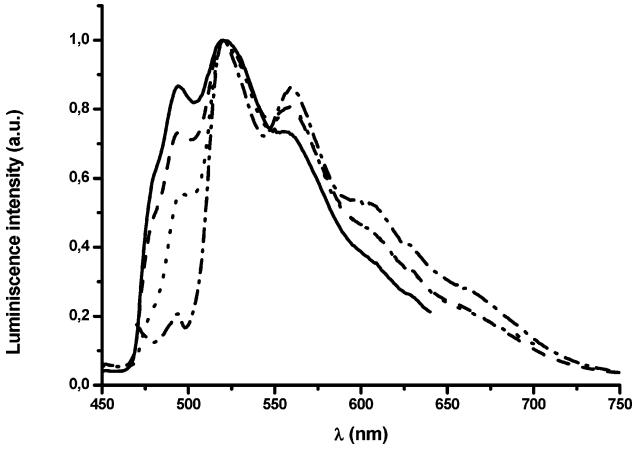

Figure 7. Normalized emission spectra of **3** in solid state at 77 K (−, excited at 330 nm; - - -, excited at 360 nm; ···, excited at 400 nm; ·—·, excited at 450 nm).

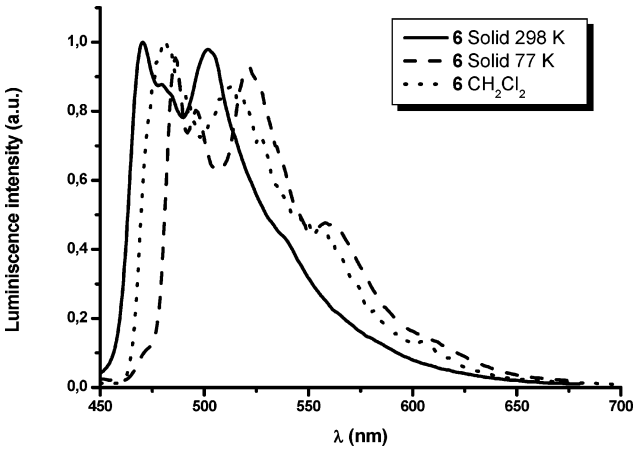

Figure 8. Normalized emission spectra of **6** in solid state at 298 K (−, λ_{ex} 390), at 77 K (- - -, λ_{ex} 390), and in CH_2Cl_2 glass at 77 K (···, λ_{ex} 360).

Figure 6, complex **1** displays in solid state a slightly structured and high-energy broad band (489 sh, 508 nm max) with a tail to lower energies and a second structured, low-energy band with a maximum at 634 and 693 nm. A similar pattern is observed for complex **3** in solid state. For both complexes, the decays of the high-energy band measured at each vibronic peak maximum are in the range of microseconds (14 μs for **1** and 10 μs for **3**) indicative of metal complex phosphorescence. The low-energy band displays a longer lifetime (110 μs **1**, 142 μs **3**). Upon cooling at 77 K, the emission profile of **1** became intensified and clearly structured with maxima shifted to lower energies (506, 544 nm). For complex **3** (see Figure 7), excitation at 450 nm resulted in a structured emission with a maximum starting at 520 nm, while by exciting at higher energies (330−400 nm), a structured emission with a high-energy component located at 497 nm was observed suggesting the presence of different emitting states. Interestingly, the low and long life energy bands observed in the solid state are not seen in frozen CH_2Cl_2 glasses, suggesting that they could be due to excimeric species resulting from the aromatic stacking between the bzq rings. In these complexes, the high-energy emission is tentatively assigned to mixed ligand-centered (^{3}LC) and metal-to-ligand charge-transfer (^{3}MLCT) transitions.[27,30,31] As shown in Figure 8, the cationic complex **6** shows, in solid state, a structured emission profile, which is red-shifted at 77 K (see Table 7) and has a vibronic spacing (1356 cm^{-1}, 298 K; 1419 cm^{-1}, 77 K) related to the skeletal stretching of the bzq ligand, suggesting its implication in the excited emissive state. This cationic complex has an exceptionally long lifetime of 189 μs in solid state at room temperature. Similar long lifetimes have been observed in other cationic and neutral platinum complexes containing the

Table 7. Photophysical Data for Platinum Complexes in Solid State and in CH_2Cl_2 Solutions

compd		λ_{max}^{em}/nm	τ/μs
[Pt(bzq)Cl(PPh_2H)] **1**	solid (298 K)	489, 508 (max) (tail to 600), 634, 693 (λ_{ex} 340−480)	14 (508) 110 (634)
	solid (77 K)	506, 544, 595 (sh) (tail to 700) (λ_{ex} 340−480)	
	CH_2Cl_2 5 × 10^{-4} M (77 K)	474 (sh), 506 (tail to 650) (λ_{ex} 390)	
[Pt(bzq)Cl($PPh_2C{\equiv}CPh$)] **3**	KBr (298 K)	510, 620 (sh) (tail to 690) (λ_{ex} 340−480)	
	solid (298 K)	494 (sh), 520 (max) (tail to 600), 629 (λ_{ex} 360−460)	10 (520) 142 (629)
	solid (77 K)	497, 520 (max), 560, 605 (sh), 626 (sh), 650 (sh) (λ_{ex} 330−400) 520, 560, 605, 626, 650 (λ_{ex} 450)	
	CH_2Cl_2 10^{-3} M (77 K)	474 (sh), 497, 535, 577 (sh), 627 (sh) (tail to 700) (λ_{ex} 340−460)	
[Pt(bzq)($PPh_2C(Ph)C(H)PPh_2$)]ClO_4 **6**	crystalline solid (298 K)	470, 479, 502, 548 (sh) (tail to 650) (λ_{ex} 390)	189 (470, 502)
	solid (77 K)	486, 501, 522, 562 (tail to 650) (λ_{ex} 320−390) 502, 540 (tail to 650) (λ_{ex} 450)	
	CH_2Cl_2 5 × 10^{-4} M (77 K)	480, 513, 560 (tail to 650) (λ_{ex} 340−440)	
[Pt(bzq)(C≡CPh)($PPh_2C{\equiv}CPh$)] **7a**	solid (298, 77 K)	no emissive	
	CH_2Cl_2 (77 K)	474 (sh), 494, 527, 567 (tail to 650) (λ_{ex} 340−440)	
[Pt(bzq)(μ-PPh_2)]$_2$ **8**	KBr (298 K)	615 (w) (λ_{ex} 400−490)	11
	solid (77 K)	602 (λ_{ex} 360−480)	

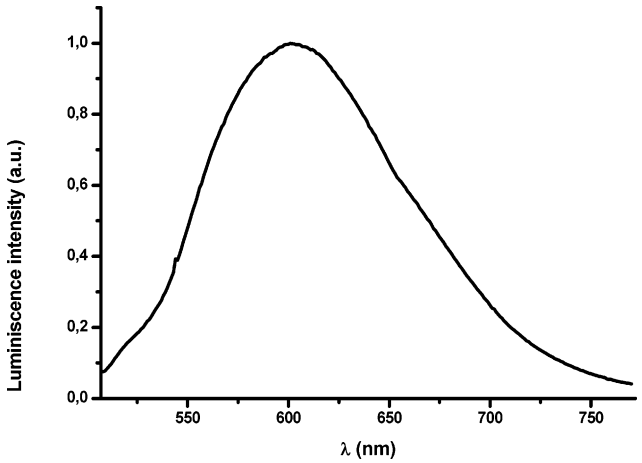

Figure 9. Normalized emission spectra of **8** in solid state at 77 K (λ_{ex} 460).

bzq ligand[15,18,30,31] and have been attributed to a higher conjugation within the π system, stabilizing the energy of the ^{3}LC excited state and thus increasing the ^{3}LC character of the emissive state. Complex **7a** is only emissive in CH_2Cl_2 glass at 77 K, displaying a structured band at a similar energy to its precursor complex **3**. Finally, the dinuclear phosphide-bridge platinum complex **8** displays a long-lived (11 μs) very weak emission at room temperature in the solid state (KBr) centered at ca. 615 nm, which is enhanced and slightly blue-shifted (602 nm) at 77 K (see Figure 9). These emissions appear clearly red-shifted compared with the mononuclear precursor **1** and are tentatively assigned to a mixture of ^{3}MLCT excited states with some $^3(\pi\pi^*)$ excimeric character due to the weak $\pi-\pi$ interactions between the bzq rings. This assignment is in agreement with the packing observed in solid state dominated by extensive intermolecular $\pi-\pi$ interactions.

Acknowledgment. We thank the Ministerio de Ciencia y Tecnología (Project No. BQU2002-03997-C02-01, 02 and a grant for A. García).

Supporting Information Available: Crystallographic data in CIF format; PLATON plots and refine structure studies of **1**, **6**, and **7b** in three different ways (model 1, with the identities of C and N as presented in this article; model 2, with the elements types reversed; model 3, with a 50/50 hybrid scattering factor at each of the affected atomic sites), pdf file. This material is available free of charge via the Internet at http://pubs.acs.org.

IC048272G